Science Press

ARTICLE

Local Structure and Dynamics Procedure of Impurities Fe, Al and Mn in Melt Beryllium

Zhang Jiqiang, Jin Lei, Luo Jiangshan, Luo Bingchi, Wu Weidong

Research Center of Laser Fusion, China Academy of Engineering Physics, Mianyang 621900, China

Abstract: The local structure and dynamics of impurities Fe, Al and Mn in beryllium were investigated on an atomic scale using ab initio molecular dynamics and statistical physics methods. The analysis of the radial distribution function centered on impurity atoms shows that the density of beryllium atoms around Fe and Mn is 8.4% and 8.6% higher than that around Al, respectively. The statistics of the measure square displacement of impurity atoms show that the diffusion coefficients of Al atoms are 114% and 133% larger than that of Fe and Mn atoms in the melt beryllium, respectively. Statistical analysis of velocity autocorrelation function of impurity atom shows that Fe and Mn atoms collide strongly with beryllium atoms in the first coordination layer, indicating that they are tightly surrounded and bound by the surrounding beryllium atoms in the central position, while the beryllium atoms around Al are loosely arranged and have weak binding forces with Al. The analysis of the activity coefficients of the impurities shows that when Fe or Mn enters the melt beryllium, it reduces the free energy of the system, whereas when Al enters, it increases the system energy. In summary, the interatomic force of BeAl is weak, so they do not form intermetallic compounds, and Al diffuses quickly in beryllium. While BeFe and BeMn have strong interatomic forces, and tend to form more BeFe and BeMn bonds to reduce the free energy of the system, so Fe and Mn diffuse slowly in beryllium. Ab initio molecular dynamics can be used to forecast the best experimental temperature for the vacuum distillation of beryllium.

Key words: beryllium; purification; ab initio molecular dynamics; local structure; activity coefficients

High-purity beryllium is often used for the P-type doping of semiconductor materials, and through the formation of PN junctions, multi-purpose devices are prepared, including the first generation of silicon devices, the second generation of GaAs, InP-based devices, the third generation of GaN, SiC, ZnO devices, etc, and in the infrared field, including the second class of superlattice devices, InSb devices, etc, it is an important doping element for the preparation of semiconductor devices. At present, high-purity beryllium has been listed as a strategic material by many countries. The outer electron configuration of the beryllium nucleus is 2, and the beryllium atom forms four covalent bonds with the surrounding four semiconductor atoms, but two holes are formed due to the lack of two valence electrons, so the doped semiconductor is a P-type semiconductor. Beryllium has the advantages of small atomic mass, easy migration to replace trivalent metals, high activation rate and various doping

forms. The beryllium acceptor in gallium nitride is the subject of intensive research at the end of the nineties. In 2013, the GaN:Be crystals were grown and a white light emitting diode was fabricated, and much higher quantum efficiency was obtained[1]. Demchenko et al[2] theoretically and experimentally addressed a possible P-type doping route of GaN using the Be acceptor. However, high-purity beryllium is difficult to obtain because the melting point of beryllium is high, and the physicochemical properties of impurity atoms vary greatly. Since the development of nuclear energy in the forties of the last century, the demand for pure beryllium has expanded rapidly. Coupled with the increase in the application of other industrial fields, the beryllium industry has developed rapidly. China, Russia as well as the United States have a considerable industrial scale of beryllium. According to the literature, the United States and the former Soviet Union prepared 99.99% high-purity beryllium. In 2011, Materion Inc (USA) released

UHP-9999 grade beryllium material, which has a purity of 99.99%, but in terms of the manufacturing process of this grade of beryllium, details of the production technique and mechanical and physical properties have seldom been reported. Vacuum distillation is an effective method for purifying beryllium metal, which has the advantages of simple equipment, short operation process and low pollution. According to public reports, both Russia and the United States have tried vacuum distillation purification method. Beryllium metal materials are strategically sensitive materials, so the key process and technique for purification are strictly blocked.

According to the results of preliminary experiments, vacuum distillation can separate most of the impurities in beryllium except Fe, Mn, etc, which are difficult to completely remove. There are some basic theoretical problems in the purification process. For instance, vapor pressure between Mn and Be is very different, so Mn is difficult to remove, while the vapor pressure between Al and Be is close and Al is easy to separate. Distillation purification includes two physical processes of volatilization and diffusion, the host metal and impurities volatilize on the melt surface, and their volatilization rates are different due to the difference in vapor pressure of different elements, thereby forming a concentration gradient of impurity in the beryllium melt. Under the action of concentration gradient, impurity atoms diffuse and migrate in the beryllium melt. The local microstructure and dynamics characteristics of different impurity atoms in the melt beryllium are key factors affecting their diffusion migration, which in turn affects their separation behavior and purification.

Ab initio molecular dynamics combines first principles with molecular dynamics simulation, directly calculates the interaction between all atoms through quantum chemical methods, and has high calculation accuracy, which is an effective method for simulating liquid metals. Molecular dynamics simulations based on a third generation of charge-optimized many body potential were performed to calculate the solid-liquid interface free energy and anisotropy of Al[3]. The effects of refractory elements on the structure and diffusivity of liquid Ni and vibrational motion of ions of $BaTiO_3$ have been investigated by ab initio molecular dynamics simulations[4–5]. To solve the dilemma of accuracy versus efficiency, interatomic potential through machine learning is proposed and has caught much attention, and the molecular dynamics simulation of the deep learning potential was used to investigate the microstructure and property of materials[6–9]. Sheng et al[10] used a combination of state-of-the-art experimental and computational techniques to resolve the atomic-level structure of amorphous alloys and elucidated different types of short-range order as well as the nature of the medium-range order. Ab initio molecular dynamics can be used to forecast the best experimental temperature for the vacuum distillation of alloys, and provides an efficient and convenient means to guide vacuum metallurgy[11]. Al, Fe and Mn are the main impurities in beryllium, and their trend and evolution in melt beryllium have typical characteristics, so they were selected as the research objects in this research. The local structure and

separate behavior of impurities Fe, Al and Mn in beryllium were investigated on atomic scale using ab initio molecular dynamics and statistical physics methods, and the relevant basic theoretical data, including the activity characteristics of impurities Al, Fe and Mn in beryllium, diffusion migration and local microstructure, etc, were clarified.

1 Computational Methods

The computer simulation in this study adopted ab initio molecular dynamics[12–16] using VASP software. The results of the molecular dynamics simulation were processed by Vaspkit software to obtain the microstructure and kinetic properties of the system. The structure was displayed by VEST software. The ion-electron interaction was described by ultra-soft Vanderbilt pseudopotentials (US-PPs) and projector augmented waves (PAWs) with a PW91 exchange-correlation function of the Brillouin zone. The simulations were performed in a canonical ensemble with fixed particle number, volume and temperature (NVT) at the Γ point, and the time step was set at 1 fs. The plane wave cut-off energy was 360 eV, and the energy convergence criterion of self-consistency was 1×10^{-4} meV/atom. The calculation accuracy was selected as normal.

The configuration in this study contains 108 atoms (107 Be atoms and 1 impurity atom), which was expressed as $Be_{107}M$ (M=Fe, Al, Mn). The initial configuration of the above system was constructed with 108 atoms randomly distributed in a cube box and equilibrated at 1573, 1673 and 1773 K by the Nose-Hoover thermostat. The densities of the molten $Be_{107}M$ alloy were obtained by test calculations. Firstly, the density of molten $Be_{107}M$ equilibrated at 1573, 1673 and 1773 K was preliminarily estimated by the theoretical density and expansion coefficient, and then the initial configuration was calculated by test. Then, based on the above initial configuration, the NPT ensemble was used to calculate the simulated cell volume under different pressures for 500 steps, with high accuracy and truncation energy of 520 eV to obtain the relationship between pressure and volume. Then, the quadratic polynomial was used to fit the pressure-volume trend line to obtain the volume under zero pressure[17–20]. The supercell volume at different pressures and temperatures is shown in Fig.1. Finally, the size and density of the simulated cell under zero pressure were calculated, which were used as the size and density of the simulated system. The size of the supercell used in the calculations and the density of each system obtained at different temperatures are listed in Table1.

Dynamics simulation ran 8000 steps at different temperatures in four systems. The last 4000 steps were analyzed by statistical physics to obtain the characteristic information of impurities in the melt beryllium, including local microstructure and dynamics characteristics.

2 Results and Discussion

2.1 Local structure

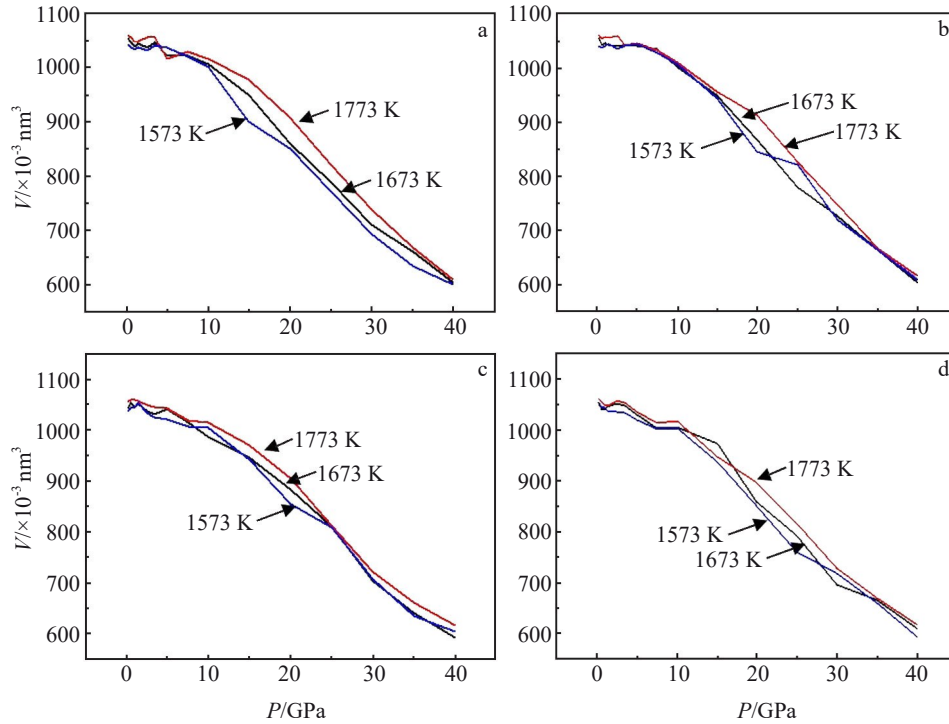Radial distribution functions are the most commonly used

Fig.1   Supercell volume at different pressures and temperatures

Table 1   Length of cube box and density of four systems at different temperatures under zero pressure

System	Temperature/K	Length/nm	Density/g·cm^{-3}
Be$_{108}$	1573	1.0192	1.533
	1673	1.0199	1.529
	1773	1.0203	1.528
Be$_{107}$Fe	1573	1.0177	1.613
	1673	1.0187	1.609
	1773	1.0217	1.595
Be$_{107}$Al	1573	1.0186	1.564
	1673	1.0205	1.555
	1773	1.0218	1.549
Be$_{107}$Mn	1573	1.0191	1.605
	1673	1.0201	1.601
	1773	1.0218	1.593

mathematical language for describing the microstructure of liquid and amorphous materials. The radial distribution function $g_{AB}(r)$ represents the probability of finding class B atoms in a spherical shell with a distance of r from the central atom of class A and a thickness of δ_r, and the ratio of the probability when class B atoms are evenly distributed throughout the simulated system. $g_{AB}(r)$ can be used to get the structural information of the system, such as atomic radius, average spacing between atoms and coordination number, so as to obtain the interrelationship between class A atoms and class B atoms. $g_{AB}(r)$ is defined as Eq.(1)[21–23]:

$$g_{AB}(r) = \frac{L^3}{N_A N_B} \left< \sum_{i=1}^{N_A} \frac{n_{iB}(r)}{4\pi r^2 \Delta r} \right> \tag{1}$$

where A and B are particle types; N_A and N_B are the number of A particles and B particles, respectively; $n_{iB}(r)$ is the number of B particles in the $(r, r+\delta_r)$ spherical shell centered on A particles.

The last 4000 frames of the trajectory of the molecular dynamics simulation were analyzed, and the radial distribution function centered on the impurity atoms Fe, Al and Mn was obtained in Fig. 2. In the radial distribution function curve, the strength of the first peak reflects the strength of the bond between the impurity atom and the Be atom. It can be seen that the first peak strengths of Be$_{107}$Fe and Be$_{107}$Mn are relatively large, that of Be108 is in the middle, and that of Be$_{107}$Al is the smallest, indicating that Be atoms centered on the Fe and Mn are tightly stacked, and the bond of BeFe and BeMn is strong, while the Be atoms centered on the Al are stacked loosely, and the bond of BeAl is weak[24]:
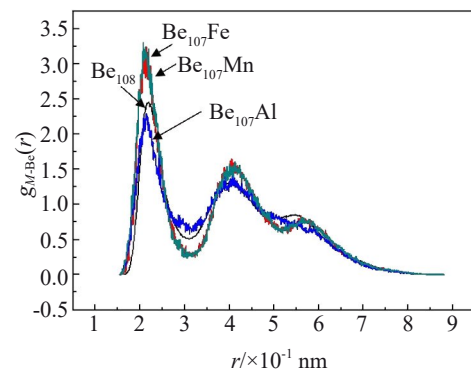

Fig.2   Radial distribution function of four impurity systems at 1673 K

$$N_{AB} = \int_0^{r_{min}} 4\pi\rho_B r^2 g_{AB}(r)\,dr \tag{2}$$

The coordination number $N_{M\text{-}Be}$ of the impurity atom Fe, Al and Mn is calculated by Eq.(2). To express the compactness of the cluster of class B atoms centered on class A atoms, the atomic number density ρ_{AB} is defined as the density of the number of class B atoms in a sphere with radius r_{min} from the central atoms of class A, calculated as[18]:

$$\rho_{AB} = \frac{N_{AB}}{4/3\pi r^3} \tag{3}$$

So far, the structural parameters of melt beryllium are calculated, including the first peak radius r_{max}, the first valley radius r_{min}, the coordination number $N_{M\text{-}Be}$ and the atomic number density $\rho_{M\text{-}Be}$, as shown in Table 2. The results show that the Be atoms centered on the Fe and Mn atoms are compact, and the Be atoms centered on the Al atoms are loose.

2.2 Dynamics characteristics

2.2.1 Mean square displacement

The diffusion coefficient of the impurities Fe, Mn and Al in melt beryllium was calculated by the mean squared

displacement (MSD) method with the Einstein equation[25–27]:

$$D = \lim_{t \to \infty} \frac{1}{6Nt}\left[\sum_{i=1}^{N}\left[r_i(t) - r_i(0)\right]^2\right] \tag{4}$$

where $r_i(0)$ and $r_i(t)$ are the coordinates of particle i at the arbitrary origin of time and t later, respectively. The MSD curves of the impurity atom Fe, Mn and Al within 4000–4500 fs, 5000–5500 fs, 6000–6500 fs and 7000–7500 fs at 1673 K are shown in Fig. 3. In this statistic, the displacement of the same impurity atom was tracked and analyzed. Statistics at different durations of the same impurity atom are independent, equivalent to statistics for large groups of particles. To improve the statistical accuracy and to avoid the influence of statistical noise, the diffusion coefficient is calculated every 500 steps (0.5 ps) and the total average values are obtained. It can be seen that Al atoms move the most rapidly in melt beryllium, while Fe atoms move slow and Mn atoms move the slowest. The diffusion coefficients of the impurities Fe, Mn and Al in melt beryllium at 1673 K calculated according to Eq.(4) are shown in Table 3. The diffusion coefficients of Fe, Mn, and Al atoms in melt beryllium at 1673 K are 3.67×10^{-3}, 3.37×10^{-3}, and 7.87×10^{-3} nm^2/ps, respectively. The results

Table 2 r_{max}, r_{min}, $N_{M\text{-}Be}$ and $\rho_{M\text{-}Be}$ of the three systems at different temperatures

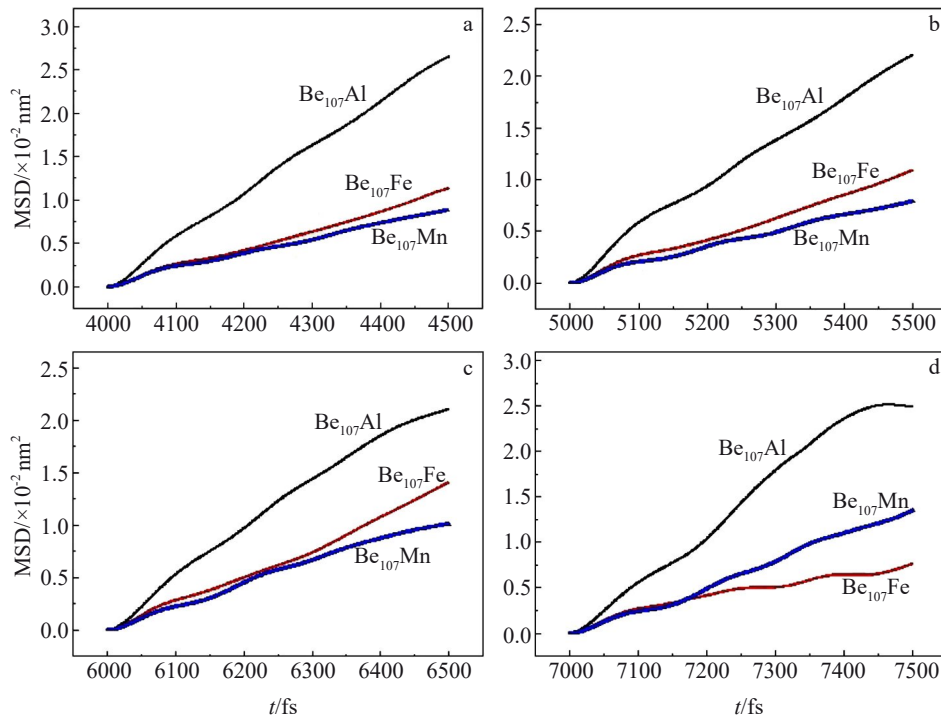| System	Be$_{107}$Fe		Be$_{107}$Al		Be$_{107}$Mn	
	1573 K	1773 K	1573 K	1773 K	1573 K	1773 K
r_{max}	2.2785	2.2782	2.5281	2.5124	2.3174	2.3813
r_{min}	3.2330	3.2459	3.4265	3.4221	3.2829	3.2853
$N_{M\text{-}Be}$	14.66	14.12	15.87	15.48	14.90	15.14
$\rho_{M\text{-}Be}$/$\times10^3$ $N\cdot$nm^{-3}	0.10357	0.09857	0.09417	0.09222	0.10050	0.10193

Fig.3 MSD of four independent statistics within different durations at 1673 K: (a) 4000–4500 fs, (b) 5000–5500 fs, (c) 6000–6500 fs, and (d) 7000–7500 fs

Table 3   MSD and diffusion coefficient (*D*) of impurities Fe, Mn, and Al in melt beryllium at 1673 K

Impurity	Fe				Mn				Al			
MSD/$\times 10^{-2}$ nm^2	1.13	1.09	1.40	0.76	0.88	0.79	1.01	1.36	2.64	2.20	2.10	2.49
Average MSD/$\times 10^{-2}$ nm^2		1.10				1.01				2.36		
D/$\times 10^{-3}$ nm^2·ps^{-1}		3.67				3.37				7.87		

show that Al diffuses rapidly in melt beryllium, while Fe and Mn diffuse slowly. The dynamics analysis of the impurity atoms is consistent with the abovementioned local microstructure analysis. In the melt beryllium, the beryllium atoms around the Al atom are loosely arranged and the binding force is weak, so Al diffuses quickly. The beryllium atoms around Fe and Mn atoms are closely arranged and have strong binding forces, so Fe and Mn diffuse slowly.

2.2.2   Velocity autocorrelation function

The time correlation function is an important quality of thermodynamic systems, which indicates the degree of correlation between a specific physical quantity at the current moment and a physical quantity at an earlier time, reflecting the causal relationship between them, and it is closely related to the migration and mass transfer process of thermodynamic system. The velocity autocorrelation function (VACF) is defined as the correlation degree of the current velocity of a particular atom in a simulated system with the velocity at an earlier time[28]:

$$VACF(t) = V_i(t_0) \cdot V(t_0 + t) \tag{5}$$

In this experiment, to improve the statistical accuracy and to avoid the influence of statistical noise, VACF statistics were performed at different time starting points for the same impurity atom, and the periods of four independent statistics

are 4000–4500 fs, 5000–5500 fs, 6000–6500 fs and 7000–7500 fs, as shown in Fig.4. It can be seen that the velocity of the impurity atom is completely autocorrelated at *t*=0, and the VACF value is 1. When *t* is greater than 0, the autocorrelation of the atom quickly disappears, decays to 0, and then oscillates rapidly with a large margin. It indicates that the impurity atom loses all momentum after a strong collision and bounces in the opposite direction of the pre-collision momentum. VACF reflects the momentum exchange of impurity atom when it collides with the surrounding Be atoms, which is only related to the characteristics of Be atoms with direct collision and momentum exchange in the first coordination layer, and has less relationship with the characteristics of Be atoms outside the first coordination layer where no direct momentum exchange occurs and only indirect momentum exchange exists. From the four independent statistics in Fig. 4, it can be seen that Al atoms have the slowest initial velocity decay and the weakest rebound, while Fe atoms decay faster and rebound strongly, and Mn atoms decay the fastest and their rebound is the strongest. It shows that Fe and Mn are tightly wrapped in the center position by the coordination atom Be and oscillate at a higher frequency, and it is difficult to break away from the encirclement formed by the coordination atom Be. The beryllium atoms around Al are looser, the collision effect is weak, and the rebound is also
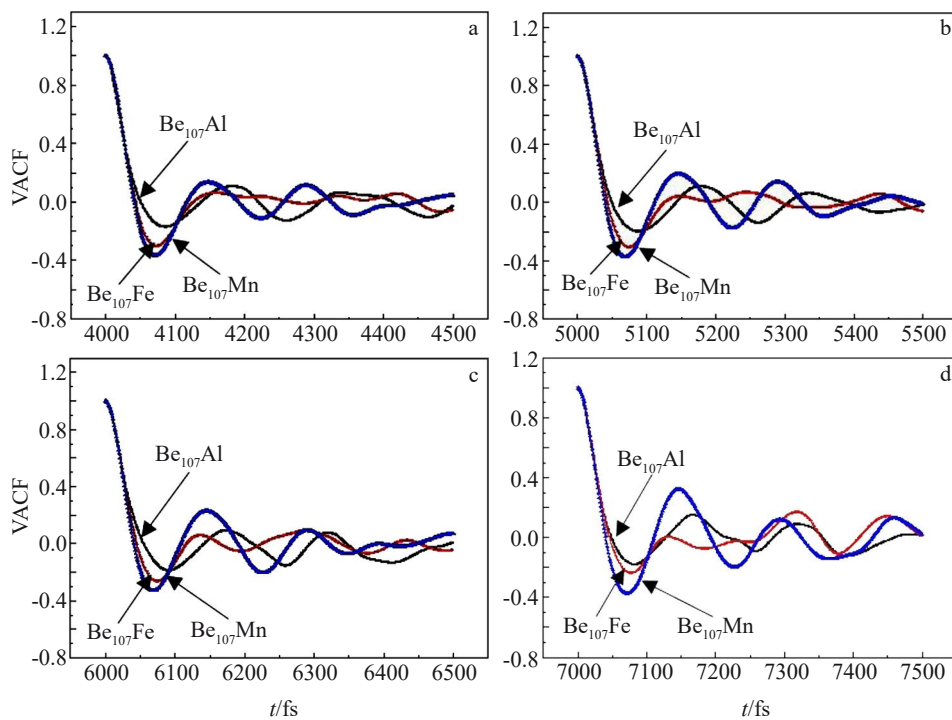

Fig.4   VACF of impurity atoms in melt beryllium at 1673 K: (a) 4000–4500 fs, (b) 5000–5500 fs, (c) 6000–6500 fs, and (d) 7000–7500 fs

Table 4   Statistics of the time when the momentum of impurity atom decays to zero at 1673 K (fs)

Impurity	Al					Fe					Mn				
	Fig.4a	Fig.4b	Fig.4c	Fig.4d	Average	Fig.4a	Fig.4b	Fig.4c	Fig.4d	Average	Fig.4a	Fig.4b	Fig.4c	Fig.4d	Average
Time	52	50	56	50	52.0	44	45	46	47	45.5	42	40	41	41	41.0

weak. The analysis of VACF is consistent with the conclusions of local microstructure analysis and diffusion coefficient analysis.

The statistics of the time when the initial momentum of the impurity atom decays to zero from abovementioned VACF are shown in Table 4. In the four statistics, the average time of the momentum of impurity atom Al, Fe and Mn decaying to zero at 1673 K is 52.0, 45.5 and 41.0 fs, respectively, indicating that the beryllium atoms around Al are loosely arranged and have weak binding forces, while the beryllium atoms around Fe and Mn are tightly arranged and have strong binding forces.

2.3 Activity characterization

In a thermodynamic system, partial molar free energy ($\partial G/\partial N$) is a quantity of strength that represents the intrinsic properties of the material system. The partial molar free energy of component i ($\partial G/\partial N_i$) has the following relationship with the activity coefficient γ_i of component i in this system[29–31]:

$$RT \ln \gamma_i = \frac{\partial G}{\partial N_i} \tag{6}$$

The activity coefficients of the impurities Fe and Al in beryllium are 0.055 and 4.71, respectively[32], thus,

$$\frac{\partial G}{\partial N_{Fe}} < 0, \quad \frac{\partial G}{\partial N_{Al}} > 0 \tag{7}$$

The intrinsic properties of the $Be_{107}M$ (M=Al, Fe, Mn) system represented by Eq.(7) are as follows. Al atom enters the beryllium matrix to increase the free energy of the system, since Al-Be interatomic attraction is less than Be-Be atomic attraction, Al atom has the effect of repelling beryllium matrix, and the system tends to form less Al-Be bonds to reduce energy. Al and Be are not miscible and do not form intermetallic compounds. When Fe atom enters the beryllium matrix, the free energy of the system decreases, the attraction between Fe and Be atoms is greater than that between Be and Be atoms, Al atoms have the effect of shrinking the beryllium matrix, the system tends to form more Fe-Be bonds to reduce energy, and finally Fe and Be are easy to form solid solutions or intermetallic compounds.

There is no interatomic activity coefficient of Be and Mn in the references, and the data are insufficient, so only qualitative estimation can be made. According to the theoretical results of this study, the interaction force between BeMn atoms is stronger than that between BeBe and MnMn, which is a negative deviation, and this kind of state is characterized by the existence of solid solutions and compounds below the liquidus line. Although the vapor pressure of Be and Mn is very different, it has a strong force with Be. In the vacuum distillation process, Mn is separated by accumulation in the residue.

3 Conclusions

1) The outer electronic structure of atom determines characteristics of interaction force between atoms. The interaction forces between Be and Al are weaker than that between Be and Be, so the system tends to form fewer BeAl bonds to reduce the system energy. Al tends to be immiscible with beryllium and does not form intermetallic compounds. In the melt beryllium, the Be atoms around the Al are stacked loosely, and thus Al diffuses and migrates quickly.

2) The interaction force between Be and Fe/Mn is stronger than that between Be and Be. The system tends to form more BeFe and BeMn bonds to reduce the free energy of the system. Fe and Mn are easy to form intermetallic compounds or solid solutions with beryllium. In melt beryllium, Fe or Mn atoms are tightly wrapped and bound by the surrounding Be atoms, so they diffuse and migrate slowly.

3) Ab initio molecular dynamics can be used to forecast the best experimental temperature for the vacuum distillation of beryllium. It provides an efficient and convenient means to guide the purification of beryllium.

References

1 Teisseyre H, Bockowski M. *Applied Physics Letters*[J], 2013, 103: 011107

2 Demchenko D O, Reshchikov M A. *Applied Physics Letters*[J], 2021, 118: 142103

3 Yan R, Ma S D. *Computational Materials Science*[J], 2020, 184: 109910

4 Zhang Z, Ma J. *Computational Materials Science*[J], 2013, 77: 254

5 Zhang X H, Zhang C Y. *Physics Review B*[J], 2022, 105: 014304

6 Podgurschi V, King D J M. *Computational Materials Science*[J], 2022, 206: 111220

7 Feng T, Zhao J. *Computational Materials Science*[J], 2022, 210: 111014

8 He R, Wu H Y. *Physics Review B*[J], 2022, 105: 064104

9 Dangic D, Fahy S. *Physics Review B*[J], 2022, 106: 134113

10 Sheng H W, Luo W K. *Nature*[J], 2006, 439: 419

11 Shi L, Jia L. *Vacuum*[J], 2023, 210: 111877

12 Kresse G, Hafner J. *Physics Review B*[J], 1994, 49: 14251

13 Alemany M M G, Gallego L J. *Physics Review B*[J], 2004, 70: 134206

14 Jakse N, Pasturel A. *Physics Review B*[J], 2014, 89: 174302

15 Andolina C M, Saidi W A. *Computational Materials Science*[J], 2022, 209: 111384

16 Steneteg P, Hellman O. *Physics Review B*[J], 2013, 87: 094114

17 Woodward C, Asta M. *Journal of Applied Physics*[J], 2010, 107:

113522

18　Yang J, Zhang J. *Computational Materials Science*[J], 2015, 109: 41

19　Yang J, Ma J B. *Computational Materials Science*[J], 2020, 175: 109611

20　Fang H Z, Wang W Y. *Physical Review B*[J], 2012, 85: 014207

21　Allen M P, Tildesley D J. *Computational Simulation of Liquids*[M]. Oxford: Clarendon Press, 1987

22　Fang H Z, Wang W Y. *Physical Review B*[J], 2012, 85: 014207

23　Hui X, Fang H Z. *Acta Materialia*[J], 2009, 57: 376

24　Gao R, Hui X. *Computational Materials Science*[J], 2008, 44: 802

25　Lin Zonghan. *Thermodynamics and Statistical Physics*[M]. Beijing: Peking University Press, 2007: 574 (in Chinese)

26　Mendelev M I, Mishin Y. *Physics Review B*[J], 2009, 80: 144111

27　Zu Z, Chen D. *Computational Materials Science*[J], 2022, 208: 111349

28　Yan Liuming, Zhu Suhua. *Theory and Practice of Molecular Dynamics Simulation*[M]. Beijing: Science Press, 2013: 174 (in Chinese)

29　Sun L. *Journal of Molecular Liquids*[J], 2022, 349: 118123

30　Chapman W G, Fouad W A. *Ind Eng Chem Res*[J], 2022, 61: 17644

31　Passamonti F J, Chialvo M R G D. *Fluid Phase Equilibria*[J], 2022, 559: 113464

32　Dai Yongnian, Yang Bin. *Vacuum Metallurgy of Non-ferrous Metal Materials*[M]. Beijing: Metallurgical Industry Press, 2000: 47 (in Chinese)

熔体铍中杂质Fe、Al和Mn的局域结构和动力学过程

张吉强，金　雷，罗江山，罗炳池，吴卫东

(中国工程物理研究院 激光聚变研究中心，四川 绵阳 621900)

摘　要：采用从头算分子动力学和统计物理方法，从原子尺度上研究了铍中杂质Fe、Al和Mn的局域结构和动力学过程。以杂质原子为中心的径向分布函数分析表明，Fe和Mn周围的铍原子密度分别比Al周围的铍原子密度高8.4%和8.6%。杂质原子平方位移的测度统计表明，熔融铍中Al原子的扩散系数分别比Fe和Mn原子大114%和133%。杂质原子速度自相关函数的统计分析表明，Fe和Mn原子在第一配位层与铍原子发生强烈碰撞，表明它们在中心位置被周围的铍原子紧密包围和束缚，而Al周围的铍原子排列松散，与Al的结合力较弱。杂质活度系数分析表明，当Fe或Mn进入熔体铍时，它降低了体系的自由能，而当Al进入时，它增加了体系能量。综上所述，BeAl原子间作用力较弱，因此它们不会形成金属间化合物，并且Al在铍中扩散迅速。而Be-Fe和Be-Mn具有很强的原子间作用力，并且倾向于形成更多的BeFe和BeMn键以降低体系的自由能，因此Fe、Mn在铍中扩散缓慢。从头算分子动力学可用于预测铍真空蒸馏的最佳实验温度。

关键词：铍；纯化；从头算分子动力学；局域结构；活度系数

作者简介：张吉强，男，1985年生，硕士生，中国工程物理研究院激光聚变研究中心，四川 绵阳 621900，电话：0816-2480872，E-mail：zhangjq383@126.com